Optim Eng (2014) 15:837–854
DOI 10.1007/s11081-013-9238-2

Considering dynamic Pareto frontiers in decision making

Patrick K. Lewis · Morgan W.P. Tackett · Christopher A. Mattson

Received: 6 April 2012 / Accepted: 24 July 2013 / Published online: 8 November 2013

Abstract Considering how the resolution of conflicts changes over time is an aspect of multiobjective optimization that is not commonly explored. These considerations embody changes in both the preferences that dictate the selection of Pareto designs, and changes in the Pareto frontier itself over time, or s-Pareto frontier when a *set* of disparate design concepts are considered. As such, this paper explores the idea of dynamic s-Pareto frontiers and preferences. Specifically, this paper presents a dynamic multiobjective optimization problem formulation that provides a framework of identifying the s-Pareto frontier for a series of time steps. The application of the presented dynamic formulation is illustrated through a simple aircraft design example. Through this example it was observed that the identification of the dynamic s-Pareto frontier enabled the observation of the impact of design decisions on the offset of selected designs from the identified dynamic frontier. By measuring and minimizing the aircraft design offset, the selected aircraft design offset was improved by an average of roughly 60 % from the next best selected alternative identified using traditional selection methods.

Keywords Multiobjective optimization · s-Pareto frontier · Dynamic multiobjective problem formulation · Decision making

Nomenclature

μ Vector of design objectives
x Vector of design variables/objects
y Vector of independent design objects
z Vector of dependent design objects

P.K. Lewis · M.W.P. Tackett · C.A. Mattson (✉)
Dept. of Mechanical Engineering, Brigham Young University, Provo, UT 84602, USA
e-mail: mattson@byu.edu

$n_{[\,]}$ indicates the number of [ ]
$[\,]_l$ indicates the lower limit of [ ]
$[\,]_u$ indicates the upper limit of [ ]
$[\,]^*$ indicates the optimal value of [ ]

1 Introduction

Engineering design is a multifaceted decision making process that often involves several conflicting design objectives. One facet that is not commonly considered is how the resolution of conflicts changes over time. That is, how to consider changes in both the preferences that dictate the selection of Pareto designs, and changes in the Pareto frontier itself over time, or s-Pareto frontier in the case where a *set* of disparate design concepts are considered. When developing a single product for multiple scenarios, a common approach in multiobjective optimization is to combine the product performance in each scenario into a single aggregate performance (Messac 2000). As a result, valuable information about the design space for individual scenarios is lost, and the effect of design decisions on the performance of a product in a given scenario is difficult to interpret.

In terms of individual design scenarios, the idea of changing design selection due to changes in preference is illustrated is Fig. 1(a) where the points $P^{(1)}$, $P^{(2)}$, and $P^{(3)}$ represent the designs selected along the Pareto frontier (bold line) at times 1, 2, and 3 respectively. Recognizing that Pareto/s-Pareto frontiers, and the resulting design space, may be dynamic due to model, concept, or environmental changes, Fig. 1(b) demonstrates the concept of both dynamic s-Pareto frontiers and preferences. From these figures it is observed that in situations where these changes can be predicted, these dynamic s-Pareto frontiers and preferences can and should be considered when making design decisions in the present. Examples of situations where these changes could be predicted include changes in manufacturing cost models due to economies of scale, planned implementation of new technologies, ranges of known operating environments, and governmental performance regulation changes (i.e., gas mileage requirements of vehicles).

This paper explores the idea of dynamic s-Pareto frontiers and preferences. Specifically, what they are, how they are obtained, and how they can be used to make better decisions in the present. In order to facilitate this exploration, a discussion of multi-objective optimization and the types of changes that existing methods could address is provided in Sect. 2. Section 3 presents a new optimization formulation capable of constructing dynamic Pareto frontiers in the presence of known/predicted changes in preferences, models, concepts, and operating environment. A simple aircraft design example illustrating the implementation of the presented dynamic optimization formulation is provided in Sect. 4, followed by concluding remarks in Sect. 5.

2 Literature review

Fundamental to the concept of dynamic Pareto frontiers is the need to balance conflicting design objectives. One common method to balance design objectives is by

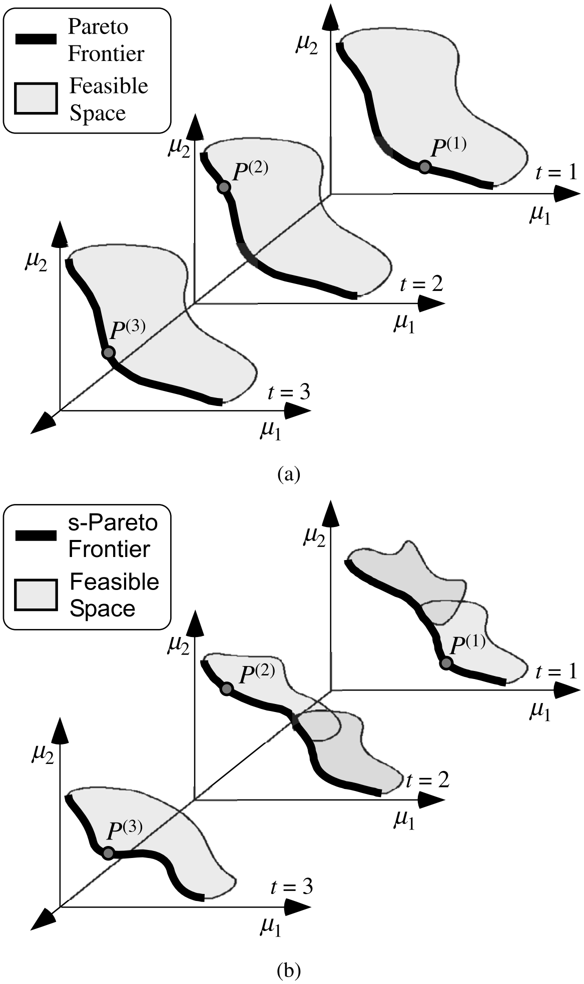

Fig. 1 (**a**) Design selections over time due to changing preference. (**b**) Design selections due to both changing preference and changing models, concepts, and/or environment

identifying non-dominated designs (Miettinen 1999; Messac and Mattson 2002) using multiobjective optimization (Yun et al. 2009; Kasprzak and Lewis 2000). The concept of non-dominance for the minimization of two objectives (μ_1 and μ_2), is represented in Figs. 1(a) and 1(b) as the Pareto/s-Pareto frontier (bold lines), where the Pareto/s-Pareto frontier characterizes the trade-offs between the objectives (Gardenghi and Wiecek 2011; Faulkenberg and Wiecek 2010).

A generic multiobjective optimization problem (MOP) formulation yielding a set of optimal solutions ($D := \{(x_1^{(k)*}, x_2^{(k)*}, \ldots, x_{n_x^{(k)}}^{(k)*})\}$)—those belonging to the s-Pareto frontier—is presented as *Problem 1 (P1)*:

$$\min_{k}\left\{\min_{x^{(k)}} \left\{\mu_1^{(k)}\left(x^{(k)}, p^{(k)}\right), \mu_2^{(k)}\left(x^{(k)}, p^{(k)}\right), \ldots, \mu_{n_\mu}^{(k)}\left(x^{(k)}, p^{(k)}\right)\right\}(n_\mu \geq 2)\right\} \quad (1)$$

Subject to $g_q^{(k)}(x^{(k)}, p^{(k)}) \leq 0$, $h_v^{(k)}(x^{(k)}, p^{(k)}) = 0$, and $x_{jl}^{(k)} \leq x_j^{(k)} \leq x_{ju}^{(k)}$. Where k denotes the k-th design concept; $\mu_i^{(k)}$ denotes the i-th generic design objective for the k-th design concept; $x^{(k)}$ is a vector of design variables for the k-th design concept; and $p^{(k)}$ is a vector of design parameters for the k-th design concept. Note that the s-Pareto frontier resulting from *P1* is a static solution, only valid at a single instance in time.

The selection of a Pareto-optimal solution typically involves the construction of an aggregate objective function that implements knowledge of the objective function parameters and sometimes constraints to capture customer needs or preferences (Messac et al. 2000; Messac 2000). Within the context of this paper, changes in Pareto solutions and preferences over time introduce unique challenges in selecting Pareto-optimal solutions. These changes can result from preference, model, concept, or environmental changes. In the context of this paper we will use the following descriptions of these sources of change:

(i) *Preferences* refer to the customer desires/needs that dictate the selection of Pareto designs (e.g., constraints, model inputs, or functions/methods of selecting a final design from a set of options).
(ii) *Models* refer to the design models used to analyze a design (e.g., analysis functions with specified inputs/outputs).
(iii) *Concepts* refer to the design concepts that the design models analyze (e.g., specific collections of analysis functions that model complete concept systems).
(iv) *Environment* refers to the operating environment of the final product/system (e.g., elements of the implementation environment that impact constraint limits and fixed model inputs).

Table 1 is provided in order to illustrate what combinations of changes have received attention in multiobjective optimization literature. Table 1 presents every possible combination of these potential sources of change, along with publications presenting methods capable of allowing for the identified combination.

It should be observed from Table 1 that publications exist that have the potential to allow for changes in concept, preference, and environment, but are for specific design approaches [e.g., modular products (Lewis and Mattson 2012; Lewis et al. 2011), families of products (Yang et al. 2004; Simpson 1998), and reconfigurable/adaptable/flexible systems (Khire and Messac 2008; Olewnik et al. 2004; Siddiqi and de Weck 2008)]. In addition, it should be observed that no publications/methods exist for combinations that contain changes in design models. This gap in publications is in part due to the form of the traditional MOP described earlier, and the inherent difficulty this formulation has in adapting to an evolving design problem as described in Curtis et al. (2013). Although changes in preferences and environments would not generally result in changes in analysis models, a formulation that enables changes in concepts would potentially need to adapt to new models introduced by the identification of new concepts. As such, a new MOP formulation that efficiently identifies a dynamic s-Pareto frontier resulting from changes in preference, model, concept, and environment is needed.

Table 1 Presentation of potential sources of change (columns 1–4) and publications (column 5) that allow for the indicated sources of change. For each combination, only sources of change with an "x" in the corresponding column are considered to change

Sources of change				Publications	
Preference	Model	Concept	Environment	Y/N	Citations
x	x	x	x	N	–
x	x	x		N	–
x	x		x	N	–
x		x	x	Y	Lewis and Mattson (2012) Yang et al. (2004) Simpson (1998)
	x	x	x	N	–
x	x			N	–
x		x		Y	Lewis and Mattson (2012) Yang et al. (2004) Simpson (1998)
x			x	Y	Lewis and Mattson (2012) Lewis et al. (2011) Yang et al. (2004) Simpson (1998)
	x	x		N	–
	x		x	N	–
		x	x	Y	Lewis and Mattson (2012) Yang et al. (2004) Simpson (1998)
x				Y	Lewis and Mattson (2012) Lewis et al. (2011) Yang et al. (2004) Simpson (1998)
	x			N	–
		x		Y	Yang et al. (2004) Simpson (1998)
			x	Y	Khire and Messac (2008) Olewnik et al. (2004) Siddiqi and de Weck (2008) Blackwell and Branke (2004) Hatzakis and Wallace (2006) Trautmann and Mehnen (2009)
				Y	Traditional MOP

3 Dynamic s-Pareto frontier formulation

The problem formulation presented in this section builds on the recent developments in dynamic MOP formulations presented in Curtis et al. (2013). Specifically, Curtis et al. (2013) focused on design space exploration in early stages of design, and demonstrated the efficiency of using a dynamic MOP with evolving design problems. The dynamic MOP presented in this section alters the dynamic MOP presented in Curtis et al. (2013) to enable the change from exploring the design space, to identifying the dynamic s-Pareto frontier for a series of known sources of change combinations. Quickly identifying the dynamic s-Pareto frontier then enables and encourages its use to guide and improve design decisions.

As MOP formulations change, what was a design parameter in one formulation could be an inequality constraint in the next formulation. Thus to avoid confusion, any variable, parameter, constraint, or objective associated with a design is termed a *design object* (Curtis et al. 2013). With this understanding, a generic dynamic multi-objective optimization problem capable of identifying the dynamic s-Pareto frontier, $D_{\mathrm{a}} := \{(x_1^{(k^{(t)})*}, \ldots, x_{n_x^{(k^{(t)})}}^{(k^{(t)})*}) | \forall t \in (1, 2, \ldots, n_t)\}$, is presented as *Problem 2 (P2)*:

$$\min_{k^{(t)}} \Big\{ \min_{y^{(k^{(t)})}} \{\mu_1^{(k^{(t)})}(x^{(k^{(t)})}), \ldots, \mu_{n_\mu^{(k^{(t)})}}^{(k^{(t)})}(x^{(k^{(t)})})\}(n_\mu^{(k^{(t)})} \geq 2)\Big\}\{k = 1, \ldots, n_k^{(t)}\} \tag{2}$$

subject to:

$$x_{l,i}^{(k^{(t)})} \leq x_i^{(k^{(t)})} \leq x_{u,i}^{(k^{(t)})} \quad \{i = 1, \ldots, n_x^{(k^{(t)})}\} \tag{3}$$

where:

$$\mu^{(k^{(t)})} = \chi^{(k^{(t)})} \cdot x^{(k^{(t)})} \tag{4}$$

$$\chi^{(k^{(t)})} = \begin{bmatrix} \chi_{1,1}^{(k^{(t)})} & \cdots & 0 \\ \vdots & \ddots & \vdots \\ 0 & \cdots & \chi_{n_x^{(k^{(t)})}, n_x^{(k^{(t)})}}^{(k^{(t)})} \end{bmatrix} \tag{5}$$

$$x^{(k^{(t)})} = \Big[y_1^{(k^{(t)})}, \ldots, y_{n_y^{(k^{(t)})}}^{(k^{(t)})}, z_1^{(k^{(t)})}(y^{(k^{(t)})}), \ldots, z_{n_z^{(k^{(t)})}}^{(k^{(t)})}(y^{(k^{(t)})})\Big]^T \tag{6}$$

$$n_x^{(k^{(t)})} = n_y^{(k^{(t)})} + n_z^{(k^{(t)})} \tag{7}$$

where $x^{(t)}$ is a vector composed of independent ($y^{(k^{(t)})}$) and dependent ($z^{(k^{(t)})}$) design objects at time step t; and the objectives identifier matrix, $\chi^{(k^{(t)})}$, is a diagonal matrix for time step t, where $\chi_{i,i}^{(k^{(t)})} \in \{-1, 0, 1\}$.

It should be noted that, with a few exceptions, *P2* is very similar to the generic s-Pareto MOP formulation (*P1*) presented in Sect. 2. For instance, the nature of x has changed to include independent and dependent design objects. In *P1*, x only contained independent design variables. The role of each design object is determined by

Table 2 Conditions for specifying design objects and object limits

Design object x_i	Condition
Minimized objective	$\chi_{i,i}^{(k^{(t)})} = 1$
Maximized objective	$\chi_{i,i}^{(k^{(t)})} = -1$
Non-objective	$\chi_{i,i}^{(k^{(t)})} = 0$
Inequality constraint	$x_{l,i}^{(k^{(t)})} \neq x_{u,i}^{(k^{(t)})}$ AND $i > n_y^{(k^{(t)})}$
Equality constraint	$x_{l,i}^{(k^{(t)})} = x_{u,i}^{(k^{(t)})}$ AND $i > n_y^{(k^{(t)})}$
Design variable	$x_{l,i}^{(k^{(t)})} \neq x_{u,i}^{(k^{(t)})}$ AND $i \leq n_y^{(k^{(t)})}$
Design parameter	$x_{l,i}^{(k^{(t)})} = x_{u,i}^{(k^{(t)})}$ AND $i \leq n_y^{(k^{(t)})}$

Eqs. (3)–(5), and the conditions determining a design object's behavior are summarized in Table 2 (Curtis et al. 2013). Additionally, we note that *P2* is minimized over $y^{(k^{(t)})}$ rather than $x^{(k^{(t)})}$ to ensure that the problem is mathematically valid.

It should be noted that *P1* and *P2* will yield the same s-Pareto frontier for a given t. However, the benefit of the formulation of *P2*, is that the MOP is established to be able to quickly and efficiently identify the dynamic s-Pareto frontier for all selected values of t. As such, the ability to use of this information to guide and improve design decisions is provided. In the next section, implementation of the presented dynamic formulation and the ability of the resulting dynamic s-Pareto frontier to improve design decisions is illustrated through a simple aircraft example with three design scenarios.

4 Aircraft example

This section implements the formulation presented in *P2* for an example based on numerical aircraft performance models presented in Heintz (2002) and Nigam and Kroo (2008). Motivation for this example comes from the Lockheed C-130 Hercules which has been enormously successful because the versatility of its design, which imparts the ability to perform many different tasks. Designed in 1951 to meet the needs of the Korean War (Bowman 1999), initial design requirements specified cargo capacity, the ability to take off from short airstrips, and the ability to fly slow enough for paradrops. Though different from the missions considered in the design, the C-130 has also been successfully used as a cargo transport, a refueling aircraft, a weather reconnaissance aircraft, and a combat gunship. To perform these new missions the aircraft was modified to meet these roles after being produced as standard C-130 models, providing a versatility that has made the platform a success (Smith 2001). In light of the focus of this paper and the various modifications that the C-130 has received over the years, the question arises of how the C-130 might have been designed if the many different missions this aircraft would need to perform were known and considered during the aircraft's development. Building from the concept of this question, the given example sets forth a method of illustrating how an optimization problem can be formulated to account for many different changes.

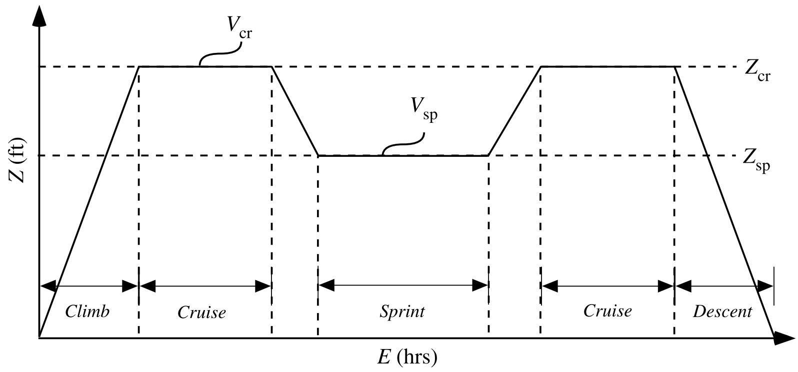

Fig. 2 Generic mission profile used to define the needed aircraft performance at different time-steps. Parameter definitions are provided in Table 4

Table 3 Summary of the concepts and objectives considered at each time-step (t)

t	Concept 1 $95 \le \varphi \le 125$ $2.2 \le C_{L,fd} \le 2.5$ $30 \le b \le 50$	Concept 2 $85 \le \varphi \le 110$ $1.8 \le C_{L,fd} \le 2.1$ $25 \le b \le 45$	Concept 3 $75 \le \varphi \le 90$ $1.5 \le C_{L,fd} \le 1.8$ $20 \le b \le 35$	Objectives
1	x	x	–	$\min\{W, P\}$
2	x	x	x	$\min\{W, P\}$
3	–	x	x	$\min\{W, P, \hat{T}_{\text{lost}}\}$

For this example all identified sources of change are considered. Changes in preference and environment are represented in three scenarios as a series of changes in the aircraft mission profile for each scenario/time-step. Figure 2 provides the generic mission profile implemented in this example. The mission parameters shown in Fig. 2 are defined with the model descriptions provided below (see Table 4).

A summary of the concepts and objectives considered at each time-step are provided in Table 3, where W is the total aircraft weight, P is a measure of the aircraft take-off/climb performance, and $\hat{T}_{\text{lost}}$ is the surveillance time lost per degree of turn. As shown in Table 3, changes in aircraft concepts are differentiated by the ranges of available engine power (φ) in billion horse power (bhp), maximum flaps down lift coefficient ($C_{L,fd}$), and the aircraft wing span (b) in feet. Changes in concepts over time are represented in Table 3 by the introduction of Concept 3 at time-step two, and the removal of Concept 1 at time-step three. Changes in model are also represented in Table 3 by the introduction of a new objective and corresponding analysis model for the final time-step. The introduction of $\hat{T}_{\text{lost}}$ as an objective in the final time-step ($t = 3$) indicates that for this mission the aircraft will be performing surveillance tasks, and consequently needs to be able to turn as quickly as possible, which assumes that no usable surveillance is captured while executing a turn.

4.1 Analysis model descriptions

To identify the s-Pareto frontiers at each time-step for the objectives identified in Table 3 requires two analysis models—application of these models differs for each concept by the ranges of the model inputs presented in Table 3. The first model calculates values of P and W, and comes from (Heintz 2002). The needed analysis functions are provided below:

$$W_{\mathrm{f}} = E \cdot r_{\mathrm{f}} \cdot \varphi \tag{8}$$

$$W_{\mathrm{u}} = W_{\mathrm{f}} + W_{\mathrm{c}} \tag{9}$$

$$W = W_{\mathrm{u}} \cdot (1 + r_{\mathrm{eu}}) \tag{10}$$

$$S_{\mathrm{fd}} = \frac{391\, W}{V_{\mathrm{s,fd}}^2 \cdot C_{\mathrm{L,fd}}} \tag{11}$$

$$S_{\mathrm{c}} = \frac{391\, W}{V_{\mathrm{s,c}}^2 \cdot C_{\mathrm{L,c}}} \tag{12}$$

$$S = \max(S_{\mathrm{fd}}, S_{\mathrm{c}}) \tag{13}$$

$$V_{\max} = 180 \sqrt[3]{\frac{\varphi}{S + 100}} \tag{14}$$

$$P = \left(\frac{W}{S}\right) \cdot \left(\frac{W}{\varphi}\right) \tag{15}$$

$$A = \frac{b^2}{S} \tag{16}$$

$$V_{\mathrm{z}} = \frac{7000 \cdot \sqrt[4]{A}}{W/\varphi} \tag{17}$$

$$Z_{\max} = 16 \cdot V_{\mathrm{z}} \tag{18}$$

$$\hat{V}_{\max} = \frac{1}{0.9 \cdot V_{\max}} \cdot \begin{cases} \max(V_{\mathrm{cr}}, V_{\mathrm{sp}}, V_{\mathrm{turn}}), & \text{for } t = 3 \\ \max(V_{\mathrm{cr}}, V_{\mathrm{sp}}), & \text{else} \end{cases} \tag{19}$$

$$\hat{Z}_{\max} = \frac{\max(Z_{\mathrm{cr}}, Z_{\mathrm{sp}})}{Z_{\max}} \tag{20}$$

The second model calculates values of $\hat{T}_{\mathrm{turn}}$, and comes from Nigam and Kroo (2008). The needed analysis functions are provided below:

$$\eta_{\max} = \frac{1.0752 \rho V_{\mathrm{turn}}^2 \cdot S \cdot C_{L,c}}{W - \frac{W_{\mathrm{f}}}{4}} \tag{21}$$

$$R_{\mathrm{turn}} = \frac{2.1503 V_{\mathrm{turn}}^2}{g \sqrt{\eta_{\max}^2 - 1}} \tag{22}$$

$$\hat{D}_{\mathrm{turn}} = \frac{\pi R_{\mathrm{turn}}}{180} \tag{23}$$

Table 4 Definitions of the model variables in Eqs. (8)–(24)

φ	Engine horse power (bhp)	W_f	Useful load (lbs)
E	Required endurance (hrs)	W_u	Useable weight (lbs)
r_f	Fuel consumption rate (lbs/hr-bhp)	W_c	Weight of cargo and occupants (lbs)
r_{eu}	Ratio of empty weight to usable weight (lbs/lbs)	$V_{s,fd}$	Stall velocity with wing flaps down (mph)
S_{fd}	Area of flaps down wings (ft^2)	W	Total Aircraft Weight (lbs)
$C_{L,fd}$	Coefficient of lift with wing flaps down	$C_{L,c}$	Coefficient of lift with clean wings
S_c	Area of clean wings (ft^2)	b	Wing span (ft)
S	Minimum needed wing area (ft^2)	$V_{s,c}$	Stall velocity of clean wings (mph)
P	Maximum takeoff/climb performance (lbs^2/ft^2-bhp)	V_{max}	Maximum possible aircraft velocity (mph)
A	Wing aspect ratio	η_{max}	Maximum aircraft load factor
$\hat{V}_{max}$	Ratio of the maximum required mission velocity to 90 % of V_{max}	V_{turn}	Aircraft Velocity while executing a turn (mph)
V_{cr}	Required mission cruise speed (mph)	V_{sp}	Required mission sprint speed (mph)
Z_{max}	Service ceiling (maximum possible flight elevation) (ft)	$\hat{Z}_{max}$	Ratio of the maximum required mission elevation to Z_{max}
Z_{cr}	Mission cruise elevation (ft)	Z_{sp}	Mission sprint elevation (ft)
g	Gravitational Constant (ft/s^2)	ρ	Density of air (lbs/ft^3)
V_z	Maximum possible rate of climb (ft/min)	R_{turn}	Minimum aircraft turn radius (ft)
$\hat{D}_{turn}$	Distance traveled per degree of turn (ft/deg)	$\hat{T}_{lost}$	Surveillance time lost per degree of turn (s/deg)

$$\hat{T}_{lost} = \frac{\hat{D}_{turn}}{V_{turn}} \tag{24}$$

where the variable definitions in the above models are given in Table 4.

4.2 Optimization results and discussion

Using the models described in Eqs. (8)–(24) and the information in Table 3, a problem of the form of *P2* was created and implemented in Matlab using the FMINCON function—a constrained nonlinear optimization solver. Design object limits and $\chi_{i,i}^{(k^{(t)})}$ values implemented in this example for each concept and time-step are summarized in Appendix A. The resulting s-Pareto frontier at each time-step is shown in Fig. 3.

From Fig. 3 it can be observed that the s-Pareto frontier changes over time as anticipated. As described in Sect. 1, the purpose of obtaining these optimal designs within each time-step is to enable better decisions to be made in the present ($t = 1$). One such decision that is required is to determine what type of aircraft will be created to account for the identified changes. Some available options would include: (i) a single non-modular/non-adjustable aircraft designed to operate in every scenario; (ii) a series of related aircraft designs that build on common platforms (product family); (iii) a reconfigurable/adjustable aircraft; or (iv) a modular aircraft that adapts to different scenarios through the addition or subtraction of modules. Recognizing that

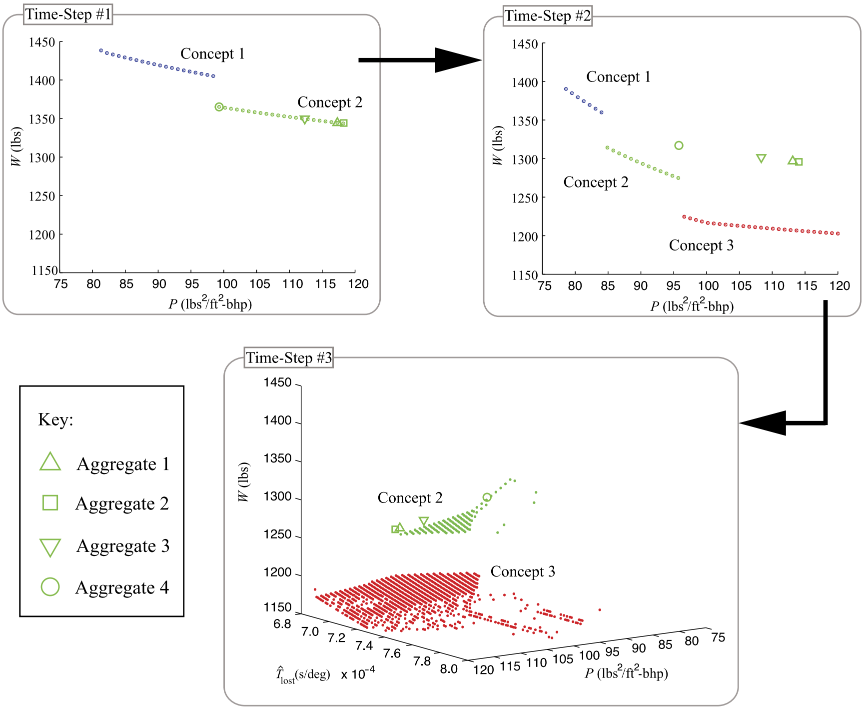

Fig. 3 Representation of s-Pareto frontier obtained for each time step using Matlab, and aircraft Concept 2 designs (△, □, ∇, and ◯) selected using four different aggregate approaches

options (ii)–(iv) require additional design methods and considerations, for this example option (i) was selected. In addition, Concept 2 was selected as the preferred concept since it appears in each time-step, and has a more moderate trade-off between W and P.

In order to select a single aircraft design for Concept 2 ($k = 2$), four different aggregate approaches were implemented. In each case, the dynamic formulation (of the form of $P2$) used to obtain the dynamic s-Pareto frontiers shown in Fig. 3 was adapted by replacing Eq. (2) in $P2$ with the following:

$$\min_{\hat{y}^{(k)}} \left\{ J\left(\mu^{(k^{(1)})}, \mu^{(k^{(2)})}, \ldots, \mu^{(k^{(n_t)})}\right) \right\} \tag{25}$$

where $\hat{y}^{(k)}$ is a vector composed of all common independent design objects ($y^{(k^{(1)})} \cup y^{(k^{(2)})} \cup \cdots \cup y^{(k^{(n_t)})}$) for the k-th design concept; and J is an aggregate objective function that combines the objective values at each time-step into a single value. Note that the formulation of J provided in Eq. (25) is generic. Specific formulations of J implemented in this example are provided in Eqs. (26), (27), (29), and (30).

The first aggregate approach used is assumed to be similar to that of the C-130, where the aircraft design was selected based on the specific requirements at one initial time. In this case, the aggregate objective function was a weighted sum of the objective values at $t = 1$ where the objective weights for P (w_P) and W (w_W) were both 0.5. Selecting a design from the previously identified s-Pareto designs at $t = 1$, the resulting performance at each time-step is represented in Fig. 3 by the symbol "△". It should be observed that the design selected at $t = 1$ is on the s-Pareto frontier. However, the performance of this design at the other time-steps ($t = 2$ and 3) is highly non-optimal due to the distance/offset of the selected design from the dynamic s-Pareto frontier. The implemented formulation of J for this approach is presented as Eq. (26) with $k = 2$ and $t = 1$.

$$J = w_P \cdot P^{(k^{(t)})} + w_W \cdot W^{(k^{(t)})} \tag{26}$$

The second aggregate approach used was to combine all objective values of a design at each time-step using a Substitute Objective Function (Cheng and Li 1996; Messac 2000) (multiplies the normalized objective values for all t together). The resulting design for this approach is represented in Fig. 3 by the symbol "□". Once again, it is observed that the design selected at $t = 1$ appears to be on the s-Pareto frontier, but the performance of this design at the other time-steps is even more non-optimal than for the first approach. The implemented formulation of J for this approach is presented as Eq. (27) with $k = 2$. Note that $\mu^{(t)*}_{\max/\min,j}$ are the max/min objective values of the identified points along the dynamic s-Pareto frontier at each time-step.

$$J = \prod_{t=1}^{3}\left(\prod_{j=1}^{n_\mu^{(t)}}\left(\frac{\mu^{(t)*}_{\max,j} - \mu^{(k^{(t)})}_j}{\mu^{(t)*}_{\max,j} - \mu^{(t)*}_{\min,j}}\right)\right) \tag{27}$$

where:

$$\mu^{(k^{(t)})} = \begin{cases} \{P^{(k^{(t)})}, W^{(k^{(t)})}, \hat{T}^{(k^{(t)})}_{\text{lost}}\}, & \text{for } t = 3 \\ \{P^{(k^{(t)})}, W^{(k^{(t)})}\}, & \text{else} \end{cases} \tag{28}$$

The third aggregate approach combined all objective values of a design at each time-step using a weighted sum. The weights used to scale the values of P ($w_P^{(t)}$) at each time-step were 0.5. The weights used to scale the values of W ($w_W^{(t)}$) at each time-step were 0.5, 0.5, and 0.3 respectively. The weight used to scale the value of $\hat{T}_{\text{lost}}$ ($w_{\hat{T}_{\text{lost}}}$) for $t = 3$ was 0.2. The resulting design for this approach is represented in Fig. 3 by the symbol "∇". Again, it is observed that the design selected at $t = 1$ appears to be on the s-Pareto frontier. However, the performance of this design at the other time-steps, although still highly non-optimal, is closer to the s-Pareto frontier than for the first two approaches. The implemented formulation of J for this approach is presented as Eq. (29) with $k = 2$.

$$J = \sum_{t=1}^{3}\begin{cases} w_P^{(t)} \cdot P^{(k^{(t)})} + w_W^{(t)} \cdot W^{(k^{(t)})} + w_{\hat{T}_{\text{lost}}} \cdot \hat{T}^{(k^{(t)})}_{\text{lost}}, & \text{for } t = 3 \\ w_P^{(t)} \cdot P^{(k^{(t)})} + w_W^{(t)} \cdot W^{(k^{(t)})}, & \text{else} \end{cases} \tag{29}$$

Note that for each of these three approaches, the design comparisons are focused around the distance/offset of these designs from the identified s-Pareto frontiers, and not simply the objective values, at each time-step. As such, a noted value of using the dynamic s-Pareto formulation is the ability to seek designs that minimize the offset

Table 5 Summary of the aircraft design offsets from the nearest s-Pareto point to the designs selected at each time-step using the four aggregate approaches (△, □, ▽, and ◯) shown in Fig. 3

t	Aggregate 1 Offsets	Aggregate 2 Offsets	Aggregate 3 Offsets	Aggregate 4 Offsets
1	0	0.08	0.65	0.03
2	22.89	23.55	19.66	11.28
3	22.83	23.47	19.58	11.29

from the dynamic s-Pareto frontier at each time-step. With this in mind, the final aggregate approach combined the offset of a given design at each time-step using a weighted sum. The weights ($\hat{w}^{(t)}$) used to scale the offset value at each time-step that resulted in the lowest offsets for $t = 2$ and 3 were 0.1, 0.75, and 0.15 respectively. The resulting design for this approach is represented in Fig. 3 by the symbol "◯". Note that the design selected at $t = 1$ appears to be on the s-Pareto frontier, and that the offsets of the selected design from the s-Pareto frontier for the remaining time-steps is significantly improved. The implemented formulation of J for this approach is presented as Eq. (30) with $k = 2$.

$$J = \sum_{t=1}^{3} \hat{w}^{(t)} \cdot \min\left(\left\|\mu_v^{(k^{(t)})*} - \mu^{(k^{(t)})}\right\| \forall v \in \left\{1, \ldots, n_\mathrm{p}^{(t)}\right\}\right) \tag{30}$$

where $\mu^{(k^{(t)})}$ is defined in Eq. (28); $\mu_v^{(t)*}$ are vectors of the identified points along the dynamic s-Pareto frontier at each time-step; and $n_\mathrm{p}^{(t)}$ is the number of $\mu^{(t)*}$ at each time-step.

It should be noted that the third aggregate approach is capable of selecting the same design as the offset approach (Aggregate 4). However, in order to maintain consistency with the weights used in Aggregate 1, this solution was not shown in Fig. 3. In addition, it is observed that the selected design for Aggregate 4 at $t = 1$ is at the limits of the s-Pareto points corresponding to Concept 2. Due to this, and the weights of Aggregate 4 required to minimize the design offsets for $t = 2$ and 3, it was concluded that the design requirements for $t = 1$ are what limits the design offset in the other scenarios. This is because the optimal aircraft design at $t = 1$ is a heavier weight aircraft than is needed in the other time-steps. As such, this is the main factor for causing offsets from the Pareto frontier for $t = 2$ and 3.

To summarize the results of the four aggregate approaches described above, Table 5 presents the offset of each approach. By comparing the information presented in Table 5 for each Aggregate Approach, the advantage of using the design offset (fourth aggregate approach) is observed. Specifically, by minimizing the design offset as in the fourth aggregate approach, there was approximately 60 % improvement over a traditional weighted sum aggregate function (third aggregate approach) that resulted in the next best selected alternative.

An additional example implementation of the presented dynamic formulation in the development of a 3/4 ton utility cart for developing nations is provided in Lewis (2012). This example describes early-stage design decisions, information gained by testing multiple prototypes, use of the problem formulation presented in this paper to understand future impacts of design decisions, and final field testing as a comparison to the optimization results. The utility cart example also indicates that the presented problem formulation is a useful design tool to explore the future impact of design decisions.

5 Concluding remarks

In response to the question of how the resolution of conflicts changes over time, this paper presented the idea of dynamic s-Pareto frontiers and preferences. Specifically, changes in both the preferences that dictate design selection, and changes in the s-Pareto frontier over time through the use of a dynamic MOP formulation was explored. The presented dynamic formulation provides a quick and efficient framework to identify the dynamic s-Pareto frontier for a selected series of scenarios/time-steps.

The application of the presented dynamic MOP formulation, and the ability to use the resulting dynamic s-Pareto frontier to guide/improve design decisions, was illustrated through a simple aircraft example for three different time-steps. Through the presented example, the simplified ability to explore a changing design space and identify the resulting dynamic s-Pareto frontier by using the dynamic s-Pareto formulation is demonstrated. In addition, the ability to use the identified dynamic s-Pareto frontier to evaluate design selections based on the offset from the frontier and thus improve design decisions is also shown. Specifically, by minimizing the aircraft design offset, the selected aircraft design offset was improved by an average of roughly 60 % from a traditional weighted sum aggregate function that resulted in the next best selected alternative.

It is observed that the use of the presented formulation can improve the ability to observe/measure the impact of design decisions on the performance of a design over time due to known changes. In considering the use of the presented formulation, it should be noted that the formulation is limited to situations where the changes that will occur over time can be predicted with reasonable accuracy. As such, application would be limited in fast paced industries where new technologies or materials are developed quickly. However, if the technology/material improvements can be predicted, then the presented formulation could be used to look beyond the current design scenario. Specifically, products could be designed to better interface with or anticipate new technologies before they are fully developed.

Acknowledgements Funding for this research was provided by the National Science Foundation Grant 0954580.

Appendix A: Dynamic s-Pareto formulation inputs

For the aircraft example given in this paper there are three concepts. The variable values for these different concepts are presented in Tables 6, 7 and 8, and were selected using data provided in Heintz (2002) for various aircraft and wing configurations. The units and descriptions of these variables are given in Table 4. The rows of the tables at each time-step are the values of the diagonal matrix ($w^{(k^{(t)})}$) and design object limits ($x_l^{(k^{(t)})}$, $x_u^{(k^{(t)})}$) for the corresponding concept. For example, the rows corresponding to $\chi_{i,i}$, x_l, and x_u for Concept 1 at $t = 1$ represent the $\chi_{i,i}^{(1^{(1)})}$ values of Eq. (5), $x_l^{(1^{(1)})}$ values of Eq. (3), and $x_u^{(1^{(1)})}$ values of Eq. (3), respectively.

Table 6 Values of the design object identifiers and limits for aircraft Concept 1 ($k = 1$)

		φ	$C_{\mathrm{L,fd}}$	$C_{\mathrm{L,c}}$	b	V_{turn}	r_{f}	r_{eu}	$V_{\mathrm{s,fd}}$	$V_{\mathrm{s,c}}$	E	W_{c}	Z_{cr}	Z_{sp}	V_{cr}	V_{sp}	g	ρ	W	P	$\hat{T}_{\mathrm{lost}}$	$\hat{V}_{\mathrm{max}}$	$\hat{Z}_{\mathrm{max}}$
$t = 1$	$\chi_{i,i}$	0	0	0	0	–	0	0	0	0	0	0	0	0	0	0	0	0	1	1	–	0	0
	x_l	95	2.2	1.1	30	–	0.40	1.4	45	50	3	450	13e3	5e3	90	120	32.2	0.0584	0	75	–	0	0
	x_u	125	2.5	1.4	50	–	0.40	1.4	45	50	3	450	13e3	5e3	90	120	32.2	0.0584	1500	120	–	1	1
$t = 2$	$\chi_{i,i}$	0	0	0	0	–	0	0	0	0	0	0	0	0	0	0	0	0	1	1	–	0	0
	x_l	95	2.2	1.1	30	–	0.40	1.4	45	50	3	430	11e3	5e3	90	110	32.2	0.0584	0	75	–	0	0
	x_u	125	2.5	1.4	50	–	0.40	1.4	45	50	3	430	11e3	5e3	90	110	32.2	0.0584	1500	120	–	1	1
$t = 3$	$\chi_{i,i}$	–	–	–	–	–	–	–	–	–	–	–	–	–	–	–	–	–	–	–	–	–	–
	x_l	–	–	–	–	–	–	–	–	–	–	–	–	–	–	–	–	–	–	–	–	–	–
	x_u	–	–	–	–	–	–	–	–	–	–	–	–	–	–	–	–	–	–	–	–	–	–

Table 7 Values of the design object identifiers and limits for aircraft Concept 2 ($k = 2$)

		φ	$C_{\mathrm{L,fd}}$	$C_{\mathrm{L,c}}$	b	V_{turn}	r_{f}	r_{eu}	$V_{\mathrm{s,fd}}$	$V_{\mathrm{s,c}}$	E	W_{c}	Z_{cr}	Z_{sp}	V_{cr}	V_{sp}	g	ρ	W	P	$\hat{T}_{\mathrm{lost}}$	$\hat{V}_{\mathrm{max}}$	$\hat{Z}_{\mathrm{max}}$
$t = 1$	$\chi_{i,i}$	0	0	0	0	–	0	0	0	0	0	0	0	0	0	0	0	0	1	1	–	0	0
	x_l	85	1.8	1.1	25	–	0.4	1.4	45	50	3	450	13e3	5e3	90	120	32.2	0.0584	0	75	–	0	0
	x_u	110	2.1	1.4	45	–	0.4	1.4	45	50	3	450	13e3	5e3	90	120	32.2	0.0584	1500	120	–	1	1
$t = 2$	$\chi_{i,i}$	0	0	0	0	–	0	0	0	0	0	0	0	0	0	0	0	0	1	1	–	0	0
	x_l	85	1.8	1.1	25	–	0.36	1.4	45	50	3	430	11e3	5e3	90	110	32.2	0.0584	0	75	–	0	0
	x_u	110	2.1	1.4	45	–	0.36	1.4	45	50	3	430	11e3	5e3	90	110	32.2	0.0584	1500	120	–	1	1
$t = 3$	$\chi_{i,i}$	0	0	0	0	0	0	0	0	0	0	0	0	0	0	0	0	0	1	1	1	0	0
	x_l	85	1.8	1.1	25	90	0.36	1.4	45	50	3.5	402	12e3	7e3	90	90	32.2	0.0584	0	75	6.9e-4	0	0
	x_u	110	2.1	1.4	45	115	0.36	1.4	45	50	3.5	402	12e3	7e3	90	90	32.2	0.0584	1500	120	8e-4	1	1

Table 8 Values of the design object identifiers and limits for aircraft Concept 3 ($k = 3$)

		φ	$C_{L,fd}$	$C_{L,c}$	b	V_{turn}	r_f	r_{eu}	$V_{s,fd}$	$V_{s,c}$	E	W_c	Z_{cr}	Z_{sp}	V_{cr}	V_{sp}	g	ρ	W	P	$\hat{T}_{lost}$	$\hat{V}_{max}$	$\hat{Z}_{max}$
$t = 1$	$\chi_{i,i}$	–	–	–	–	–	–	–	–	–	–	–	–	–	–	–	–	–	–	–	–	–	–
	x_l	–	–	–	–	–	–	–	–	–	–	–	–	–	–	–	–	–	–	–	–	–	–
	x_u	–	–	–	–	–	–	–	–	–	–	–	–	–	–	–	–	–	–	–	–	–	–
$t = 2$	$\chi_{i,i}$	0	0	0	0	–	0	0	0	0	0	0	0	0	0	0	0	0	1	1	–	0	0
	x_l	75	1.5	1.1	20	–	0.30	1.4	45	50	3	430	11e3	5e3	90	110	32.2	0.0584	0	75	–	0	0
	x_u	90	1.8	1.4	35	–	0.30	1.4	45	50	3	430	11e3	5e3	90	110	32.2	0.0584	1500	120	–	1	1
$t = 3$	$\chi_{i,i}$	0	0	0	0	0	0	0	0	0	0	0	0	0	0	0	0	0	1	1	1	0	0
	x_l	75	1.5	1.1	20	90	0.30	1.4	45	50	3.5	402	12e3	7e3	90	90	32.2	0.0584	0	75	6.9e-4	0	0
	x_u	90	1.8	1.4	35	115	0.30	1.4	45	50	3.5	402	12e3	7e3	90	90	32.2	0.0584	1500	120	8e-4	1	1

References

Blackwell T, Branke J (2004) Multi-swarm optimization in dynamic environments. Lecture Notes in Computer Science, vol 3005. pp 489–500. doi:10.1007/978-3-540-24653-4_50

Bowman MW (1999) Lockheed C-130 Hercules Crowood Press, Ramsbury, pp 4–54

Cheng FY, Li D (1996) Multiobjective optimization of structures with and without control. J Guid Control Dyn 19(2):392–397

Curtis SK, Mattson CA, Hancock BJ, Lewis PK (2013) Divergent exploration in design with a dynamic multiobjective optimization formulation. Struct Multidiscip Optim 47(5):645–657

Faulkenberg SL, Wiecek MM (2010) On the quality of discrete representations in multiple objective programming. Optim Eng 11:423–440. doi:10.1007/s11081-009-9099-x

Gardenghi M, Wiecek MM (2011) Efficiency for multiobjective multidisciplinary optimization problems with quasiseparable subproblems. Optim Eng, 293–318. doi:10.1007/s11081-011-9136-4

Hatzakis I, Wallace D (2006) Dynamic multi-objective optimization with evolutionary algorithms: a forward-looking approach. In: Proceedings of the 8th annual conference on Genetic and evolutionary computation, GECCO '06, New York, NY, USA, ACM, New York, pp 1201–1208. ISBN:1-59593-186-4. 10.1145/1143997.1144187

Heintz C (2002) Aircraft design made easy. EAA Exp. http://www.zenithair.com/images/kit-data/ht.html

Kasprzak EM, Lewis KE (2000) An approach to facilitate decision tradeoffs in Pareto solution sets. J Eng Valuat Cost Anal 3:173–187

Khire RA, Messac A (2008) Selection-integrated optimization (SIO) methodology for optimal design of adaptive systems. J Mech Des 130(10):101401

Lewis PK (2012) An optimization-based method of traversing dynamic s-Pareto frontiers. PhD thesis, Brigham Young University

Lewis PK, Mattson CA (2012) A method for developing systems that traverse the Pareto frontiers of multiple system concepts through modularity. Struct Multidiscip Optim 45(4):467–478. doi:10.1007/s00158-010-055501

Lewis PK, Murray VR, Mattson CA (2011) A design optimization strategy for creating devices that traverse the Pareto frontier over time. Struct Multidiscip Optim 43(2):191–204. doi:10.1007/s00158-010-0555-1

Messac A (2000) From dubious construction of objective functions to the application of physical programming. AIAA J 38(1):155–163

Messac A, Mattson CA (2002) Generating well-distributed sets of Pareto points for engineering design using physical programming. In: Optimization and engineering, vol 3. Kluwer Academic, Norwell, pp 431–450

Messac A, Puemi-Sukam C, Melachrinoudis E (2000) Aggregate objective functions and Pareto frontiers: required relationships and practical implications. Optim Eng 1:171–188

Miettinen KM (1999) Nonlinear multiobjective optimization. International series in operations research & management science. Kluwer Academic, Norwell, pp 5–36

Nigam N, Kroo I (2008) Control and design of multiple unmanned air vehicles for a persistent surveillance task. In: 12th AIAA/ISSMO multidisciplinary analysis and optimization conference, Victoria, British Columbia, Sep. 10–12, pp 1–14. Number AIAA-2008-5913

Olewnik A, Brauen T, Ferguson S, Lewis K (2004) A framework for flexible systems and its implementation in multiattribute decision making. J Mech Des 126(3):412–419

Siddiqi A, de Weck OL (2008) Modeling methods and conceptual design principles for reconfigurable systems. J Mech Des 130:101102

Simpson TW (1998) Product platform design and optimization: status and promise. Artif Intell Eng Des Anal Manuf 18(1):3–20

Smith PC (2001) Lockheed C-130 Hercules: the World's favourite military transport. Crowood, Wiltshire, pp 12–140

Trautmann H, Mehnen J (2009) Preference-based Pareto optimization in certain and noisy environments. Eng Optim 41(1):23–38. doi:10.1080/03052150802347926

Yang TG, Beiter KA, Ishii K (2004) Product platform development: an approach for products in the conceptual stages of design. In: 2004 ASME international mechanical engineering congress and RDD expo, pp 97–108. Number IMECE2004-62171

Yun Y, Yoon M, Nakayama H (2009) Multi-objective optimization based on meta-modeling by using support vector regression. Optim Eng 10:167–181. doi:10.1007/s11081-008-9063-1